Implication on the pion distribution amplitude from the pion-photon transition form factor with the new *BABAR* data

Xing-Gang Wu*

Department of Physics, Chongqing University, Chongqing 400044, People's Republic of China

Tao Huang†

Institute of High Energy Physics and Theoretical Physics Center for Science Facilities, Chinese Academy of Sciences, Beijing 100049, People's Republic of China

(Received 19 May 2010; published 19 August 2010)

The new *BABAR* data on the pion-photon transition form factor arouses people's interest for the determination of the pion distribution amplitude. To explain the data, we take both the leading valence quark state's and the nonvalence quark state's contributions into consideration, where the valence quark part up to next-to-leading order is presented and the nonvalence quark part is estimated by a phenomenological model based on its limiting behavior at both $Q^2 \to 0$ and $Q^2 \to \infty$. Our results show that to be consistent with the new *BABAR* data at the large Q^2 region, a broader amplitude other than the asymptoticlike pion distribution amplitude should be adopted. The broadness of the pion distribution amplitude is controlled by a parameter B. It has been found that the new *BABAR* data at low and high energy regions can be explained simultaneously by setting B to be around 0.60, in which the pion distribution amplitude is closed to the Chernyak-Zhitnitsky form.

DOI: 10.1103/PhysRevD.82.034024 PACS numbers: 12.38.−t, 12.38.Bx

I. INTRODUCTION

The pion-photon transition form factor $\gamma\gamma^* \to \pi^0$, which relates two photons with one lightest meson, is the simplest example for the perturbative application to exclusive processes. It provides a good platform to study the property of pion distribution amplitude (DA), i.e. one can extract useful information on the shape of the leading-twist pion DA by comparing the estimated result on the transition form factor $F_{\pi\gamma}(Q^2)$ with the measured one. The CELLO Collaboration measured the pion-photon transition form factor a long time ago, where one of the photons was nearly on shell and the other one was off shell with a virtuality in the range of the low energy region ($Q^2 < 3$ GeV^2) [1]. Later on, the CLEO Collaboration also measured such a form factor but with a broader range of $Q^2 \in [1.5, 9.2]$ GeV^2 [2]. Very recently, the *BABAR* Collaboration did a more precise measurement at both low and high energy regions, and their data show that in the range of $Q^2 \in [4, 40]$ GeV^2, the pion-photon transition form factor behaves as [3]

$$Q^2 F_{\pi\gamma}(Q^2) = A\left(\frac{Q^2}{10\ \text{GeV}^2}\right)^{\beta}, \tag{1}$$

where $A = 0.182 \pm 0.002$ and $\beta = 0.25 \pm 0.02$. Such large Q^2 behavior contradicts the well-known asymptotic prediction [4], i.e. $Q^2 F_{\pi\gamma}(Q^2)$ tends to be a constant ($2f_\pi$) for asymptotic DA $\phi_{\text{as}}(x, Q^2)|_{Q^2\to\infty} = 6x(1-x)$, where the pion decay constant $f_\pi = 92.4 \pm 0.25$ MeV [5]. By extending the previous next-to-leading order (NLO) corrections [6,7] to the present large Q^2 region, or even by including the next-to-next-to-leading order corrections [8,9], the significant growth of the pion-photon transition form factor between 10 and 40 GeV^2 cannot be explained by using the asymptotic or asymptoticlike DA.

Therefore, many attempts have tried to solve the present puzzle and some authors have argued that in contrary to the conventional adopted asymptoticlike DA, the pion DA should be quite broad or even flat in its whole region [10–13]. More explicitly, with a flat DA $\phi(x) \equiv 1$, Ref. [10] shows that the present *BABAR* data at large Q^2 can be explained by choosing proper values for the phenomenological parameters for the logarithmic model and the Gaussian model constructed there. However, there is no strong reason to support such a flat DA, since the introduced infrared regulator m^2 (or σ) is rightly fitted by the *BABAR* data. Moreover, one may observe that Ref. [10] fails to explain the small Q^2 behavior, and it cannot reproduce the well-known value of $F_{\pi\gamma}(Q^2 = 0) = 1/(4\pi^2 f_\pi)$ that is derived from measuring the rate of $\pi^0 \to \gamma\gamma$ [14]. Also it can be easily seen that the flat DA with the wave-function model suggested in Ref. [10] cannot derive the right behavior at $Q^2 \to 0$, since as will be shown later, it will lead to the probability of finding the valence quark state in the pion,

$$P_{q\bar{q}} = \int_0^1 \left(\frac{\pi^2 f_\pi^2}{3x(1-x)\sigma}\right) dx,$$

and the charged mean squared radius,

*wuxg@cqu.edu.cn
†huangtao@ihep.ac.cn

$$\langle r^2_{\pi^+}\rangle^{q\bar{q}} = \int_0^1 \left(\frac{\pi^2 f_\pi^2}{2x^2\sigma^2}\right) dx,$$

both of which are divergent. Furthermore, with such a flat DA, the end-point singularity shall emerge in many exclusive processes, such as $B \to$ light meson transition form factors, which makes them not calculable in perturbative QCD. This shall greatly compress the applicability of perturbative QCD.[1]

At present, there is no definite conclusion on whether pion DA is in asymptotic form [4], in Chernyak-Zhitnitsky (CZ) form [17], or even in flat form [18]. The pion DA can be expressed in Gegenbauer expansion [4]. The value of the Gegenbauer moments have been studied in various processes; cf. Refs. [19–27]. The lattice result of Ref. [27] prefers a narrower DA with $a_2(1\ \mathrm{GeV}^2) = 0.07(1)$, while the lattice results [25,26] prefer broader DA, i.e. they obtain $a_2(1\ \mathrm{GeV}^2) = 0.38 \pm 0.23^{+0.11}_{-0.06}$ and $a_2(1\ \mathrm{GeV}^2) = 0.364 \pm 0.126$, respectively. These references favor a positive value for $a_2(1\ \mathrm{GeV}^2)$ and the most recent one is done by Ref. [23], which shows that $a_2(1\ \mathrm{GeV}^2) = 0.17^{+0.15}_{-0.17}$ through a QCD light-cone sum rule analysis of the semileptonic $B \to \pi$ weak transition form factor based on the *BABAR* data on $B \to \pi l\nu$ [28]. The pion-photon transition form factor being involved in only one pion DA maybe helpful to clarify the present situation.

As argued in Ref. [14], the leading Fock state contributes to $F_{\pi\gamma}(0)$ by only one-half and the remaining one-half should come from the higher Fock states as $Q^2 \to 0$. And then both contributions from the leading Fock state and the higher Fock states are needed to get the correct $\pi^0 \to \gamma\gamma$ rate. In Ref. [29], we have made such a comprehensive analysis of the pion-photon transition form factor in a smaller Q^2 region, e.g. $Q^2 \in [0, 10]\ \mathrm{GeV}^2$, by taking both the valence quark and the nonvalence quark contributions into consideration. It has been found that both the asymptoticlike and the CZ-like DAs can explain the CELLO and CLEO data [1,2] by setting proper parameters for the pion wave function. Then it shall be interesting to extend our previous analysis to a higher Q^2 region so as to determine which pionic behavior is more preferable for consistently explaining the CELLO, CLEO, and *BABAR* data within the whole measured energy region.

The paper is organized as follows. In Sec. II, we present the calculation technology to derive the valence and nonvalence contributions to the pion-photon transition form factor. For such purpose, we construct a pion wave function model based on the Brodsky-Huang-Lepage (BHL) prescription and present all the necessary formulas for discussion of its properties. In Sec. III, we discuss what we can learn of the pionic leading Fock-state wave function/DA in comparison with CELLO, CLEO, and *BABAR* experimental data. Some further discussion and comments are made in Sec. IV.

[1]Within the $k_\perp$ factorization approach, by keeping the transverse momentum dependence consistently and with the help of the Sudakov and threshold resummation, this end-point singularity may be cured to a certain degree, e.g. for the pion-photon transition form factor [15] and for $B \to$ light form factors [16].

II. CALCULATION TECHNOLOGY

Generally, the pion-photon transition form factor $\gamma\gamma^* \to \pi^0$ can be written as

$$F_{\pi\gamma}(Q^2) = F^{(V)}_{\pi\gamma}(Q^2) + F^{(NV)}_{\pi\gamma}(Q^2), \tag{2}$$

where $F^{(V)}_{\pi\gamma}(Q^2)$ is the usual valence quark part, and $F^{(NV)}_{\pi\gamma}(Q^2)$ stands for the nonvalence quark part that is related to the higher Fock state of the pion. The valence quark contribution $F^{(V)}_{\pi\gamma}(Q^2)$ dominates only as Q^2 becomes very large. Figure 1 shows this point more clearly. $F^{(V)}_{\pi\gamma}(Q^2)$ comes from Fig. 1(a), which involves the direct annihilation of the $(q\bar{q})$ pair into two photons, i.e. the leading Fock-state contribution that dominates the large Q^2 contribution. $F^{(NV)}_{\pi\gamma}(Q^2)$ comes from Fig. 1(b), in which one photon coupling "inside" the pion wave function, i.e. strong interactions occur between the photon interactions that are related to the higher Fock-state's contributions [30]. Under the light-cone perturbative QCD approach [4], we can obtain the valence part $F^{(V)}_{\pi\gamma}(Q^2)$. While for the nonvalence part $F^{(NV)}_{\pi\gamma}(Q^2)$, because of its nonperturbative nature, we shall construct a phenomenological model based on limiting behavior at $Q^2 \to 0$ and $Q^2 \to \infty$ to estimate its contribution.

Since the pion wave function is the key component of the pion-photon transition form factor, in the following sections, we shall first have a discussion on its explicit form.

A. Pion wave function and related DA

Taking into account the Melosh rotation [31], the full form of the pion wave function can be written as

$$\Psi_{q\bar{q}}(x, \mathbf{k}_\perp) = \sum_{\lambda_1\lambda_2} \chi^{\lambda_1\lambda_2}(x, \mathbf{k}_\perp)\Psi^R_{q\bar{q}}(x, \mathbf{k}_\perp), \tag{3}$$

where λ_1 and λ_2 are the helicity states of the two constitute

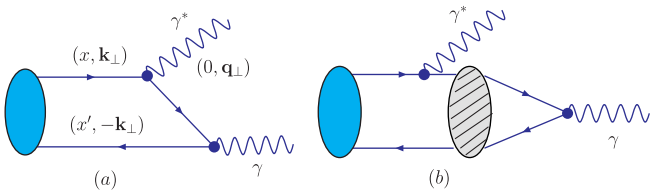

FIG. 1 (color online). Typical diagrams that contribute to the pion-photon transition form factor $F_{\pi\gamma}(Q^2)$, where $x' = (1 - x)$. The rightmost shaded oval with a slant pattern stands for the strong interactions.

quarks, and $\chi^{\lambda_1\lambda_2}(x, \mathbf{k}_\perp)$ stands for the spin-space wave function coming from the Wigner-Melosh rotation. $\chi^{\lambda_1\lambda_2}(x, \mathbf{k}_\perp)$ can be found in Refs. [32–35], whose explicit form is shown in Table I. $\Psi^R_{q\bar{q}}(x, \mathbf{k}_\perp)$ stands for the spatial wave function, and we adopt the factorized model to do our discussion, which is divided into a x-dependent part $\varphi_\pi(x)$ and a $\mathbf{k}_\perp$-dependent part. $\varphi_\pi(x)$ may or may not be the distribution amplitude, which depends on the explicit form of the $\mathbf{k}_\perp$-dependent part. Based on the BHL prescription [14,32–35], the spatial wave function $\Psi^R_{q\bar{q}}(x, \mathbf{k}_\perp)$ can be written as

$$\Psi^R_{q\bar{q}}(x, \mathbf{k}_\perp) = A\varphi_\pi(x) \exp\left[-\frac{\mathbf{k}_\perp^2 + m_q^2}{8\beta^2 x(1-x)}\right], \quad (4)$$

where the x-dependent part $\varphi_\pi(x)$ can be expanded in Gegenbauer polynomials, and by keeping its first two terms, we obtain

$$\Psi^R_{q\bar{q}}(x, \mathbf{k}_\perp) = A(1 + B \times C_2^{3/2}(2x-1)) \times \exp\left[-\frac{\mathbf{k}_\perp^2 + m_q^2}{8\beta^2 x(1-x)}\right], \quad (5)$$

where the Gegenbauer polynomial $C_2^{3/2}(2x-1) = (3/2)[5(2x-1)^2 - 1]$. The typical parameter B determines the broadness of the wave function. The normalization constant A, the harmonic scale β, and the light constitute quark mass m_q are constrained by several reasonable constraints. The first is the conventional wave-function normalization condition

$$\int_0^1 dx \int_{|\mathbf{k}_\perp|^2 < \mu_0^2} \frac{d^2\mathbf{k}_\perp}{16\pi^3} \Psi_{q\bar{q}}(x, \mathbf{k}_\perp) = \frac{f_\pi}{2\sqrt{3}}, \quad (6)$$

where μ_0 stands for some hadronic scale that is of order $\mathcal{O}(1\ \text{GeV})$. The second is the constraint derived from $\pi^0 \to \gamma\gamma$ decay amplitude [14]

$$\int_0^1 dx \Psi_{q\bar{q}}(x, \mathbf{k}_\perp = 0) = \frac{\sqrt{3}}{f_\pi}. \quad (7)$$

Furthermore, m_q should be around the conventional adopted value of 0.30 GeV.

The leading Fock-state pion DA at the scale μ_0 takes the following form:

$$\phi_\pi(x, \mu_0^2) = \frac{2\sqrt{3}}{f_\pi} \int_{|\mathbf{k}_\perp|^2 \le \mu_0^2} \frac{d^2\mathbf{k}_\perp}{16\pi^3} \Psi_{q\bar{q}}(x, \mathbf{k}_\perp). \quad (8)$$

Substituting the wave-function model (3), we obtain

TABLE I. The explicit form of the spin-space wave function $\chi^{\lambda_1\lambda_2}(x, \mathbf{k}_\perp)$.

$\lambda_1\lambda_2$	$\downarrow\downarrow$ ($\uparrow\uparrow$)	$\uparrow\downarrow$	$\downarrow\uparrow$
$\chi^{\lambda_1\lambda_2}(x, \mathbf{k}_\perp)$	$-\frac{k_x \pm ik_y}{\sqrt{2(m_q^2 + \mathbf{k}_\perp^2)}}$	$\frac{m_q}{\sqrt{2(m_q^2 + \mathbf{k}_\perp^2)}}$	$-\frac{m_q}{\sqrt{2(m_q^2 + \mathbf{k}_\perp^2)}}$

$$\phi_\pi(x, \mu_0^2) = \frac{\sqrt{3}Am\beta}{2\sqrt{2}\pi^{3/2} f_\pi} \sqrt{x(1-x)} \times (1 + B \times C_2^{3/2}(2x-1)) \times \left(\text{erf}\left[\sqrt{\frac{m^2 + \mu_0^2}{8\beta^2 x(1-x)}}\right] - \text{erf}\left[\sqrt{\frac{m^2}{8\beta^2 x(1-x)}}\right]\right), \quad (9)$$

where the error function $\text{erf}(x)$ is defined as $\text{erf}(x) = \frac{2}{\sqrt{\pi}} \times \int_0^x e^{-t^2} dt$. Such a DA with $B \to 0$ is asymptoticlike, and with the increment of B, it shall be broadened to a certain degree, e.g. when $B \sim 0.6$, it will be CZ like with a $k_\perp$-dependent factor which suppresses the end-point singularity.

The pion DA at any scale Q^2 can be derived from the initial DA $\phi_\pi(x, \mu_0^2)$ through QCD evolution. The evolution equation up to order $\mathcal{O}(\alpha_s)$ takes the following form [36]:

$$xx'Q^2 \frac{\partial \tilde{\phi}_\pi(x, Q^2)}{\partial Q^2} = C_F \frac{\alpha_s(Q^2)}{4\pi} \left\{\int_0^1 [dy] V(x, y) \tilde{\phi}_\pi(y, \mu) - xx' \tilde{\phi}_\pi(x, Q^2)\right\}, \quad (10)$$

where $[dy] = dydy'\delta(1 - y - y')$, $\tilde{\phi}_\pi(x, Q^2) = \phi_\pi(x, Q^2)/(xx')$ with $x' = 1 - x$, and

$$V(x, y) = 2C_F\left[xy'\theta(y - x)\left(\delta_{h_1\bar{h}_2} + \frac{\Delta}{y - x}\right) + (1 \leftrightarrow 2)\right],$$

where $(1 \leftrightarrow 2)$ means that all the properties of the first constitute quark should be exchanged to that of the second one, and vice versa. $\delta_{h_1\bar{h}_2} = 1$ when the two constitute quarks' helicities h_1 and h_2 are opposite and $\Delta\tilde{\phi}_\pi(y, Q^2) = \tilde{\phi}_\pi(y, Q^2) - \tilde{\phi}_\pi(x, Q^2)$. With this evolution equation, we can take the evolution effects in calculating the pion-photon transition form factor.

Moreover, a solution of Eq. (10) in Gegenbauer expansion has been derived by Ref. [36], which takes the following form:

$$\phi_\pi(x, Q^2) = 6xx' \sum_{n=0}^{\infty} a_n(\mu_0^2)\left(\ln\frac{Q^2}{\Lambda^2_{\text{QCD}}}\right)^{-\gamma_n} C_n^{3/2}(2x-1), \quad (11)$$

where the Gegenbauer polynomials $C_n^{3/2}(2x-1)$ are eigenfunctions of $V(x, y)$ and the corresponding eigenvalues are the "nonsinglet" anomalous dimensions

$$\gamma_n = \frac{C_F}{\beta_0}\left(1 + 4\sum_{k=2}^{n+1}\frac{1}{k} - \frac{2\delta_{h_1\bar{h}_2}}{(n+1)(n+2)}\right),$$

where $\beta_0 = 11 - 2n_f/3$. The nonperturbative coefficients $a_n(\mu_0^2)$ can be determined from the initial condition $\phi_\pi(x, \mu_0^2)$ by using the orthogonality relations for the

Gegenbauer polynomials $C_n^{3/2}(2x-1)$, i.e.

$$a_n(\mu_0^2) = \frac{\int_0^1 dx \phi_\pi(x,\mu_0^2) C_n^{3/2}(2x-1)}{\int_0^1 dx 6x(1-x)[C_n^{3/2}(2x-1)]^2}. \quad (12)$$

It should be noted that even though the model wave function (4) is constructed by using only the first two Gegenbauer terms in the longitudinal function $\varphi_\pi(x)$, our present DA $\phi_\pi(x,\mu_0^2)$ as shown by Eq. (9) can be expanded in a full form of Gegenbauer series, i.e. both the leading and the higher Gegenbauer terms are there, whose corresponding Gegenbauer moments can be calculated with the help of Eq. (12). As will be shown in Table II, the second Gegenbauer moment $a_2(\mu_0^2)$ is close but not equal to the parameter B. This shows that the DA ϕ_π is different from φ_π, which is due to the choice of the BHL-transverse momentum dependence and the consideration of all the helicity components' contributions. While by taking a simpler Gaussian-transverse momentum dependence and by taking only the usual helicity component into consideration, e.g. the transverse momentum dependence $\propto \exp(-\frac{k_\perp^2}{2\sigma x(1-x)})$ [10], it leads to $\phi_\pi(x,\mu_0^2) \equiv \varphi_\pi(x)$, and $a_2(\mu_0^2) = B$.

B. $F_{\pi\gamma}^{(V)}(Q^2)$ up to NLO

Under the light-cone perturbative QCD approach [4], and by keeping the $k_\perp$ corrections in both the hard-scattering amplitude and the wave function, $F_{\pi\gamma}(Q^2)$ has been calculated up to NLO [14,15,29,37–39]. It is noted that for high helicity states ($\lambda_1 + \lambda_2 = \pm 1$), since their hard parts are proportional to the small current quark mass, we can safely neglect their contributions. As a combination of the LO [14,29,37,38] and the NLO parts [15,39] that keep the $k_\perp$ dependence in the hard kernel, we can obtain the following formula after doing the integration over the azimuth angle:

$$F_{\pi\gamma}^{(V)}(Q^2) = \frac{1}{4\sqrt{3}\pi^2}\int_0^1\int_0^{x^2Q^2}\frac{dx}{xQ^2}\Big[1 - \frac{C_F\alpha_s(Q^2)}{4\pi} \times \Big(\ln\frac{\mu_f^2}{xQ^2+k_\perp^2} + 2\ln x + 3 - \frac{\pi^2}{3}\Big)\Big] \times \Psi_{q\bar{q}}(x,k_\perp^2)dk_\perp^2, \quad (13)$$

where $[dx] = dxdx'\delta(1-x-x')$, $C_F = 4/3$, and $k_\perp = |\mathbf{k}_\perp|$. μ_f stands for the factorization scale, and for convenience, we take $\mu_f = Q$ [6,7]. Here, without loss of generality, the usual assumption that the pion wave function depending on $\mathbf{k}_\perp$ through $k_\perp^2$ only, i.e. $\Psi_{q\bar{q}}(x,\mathbf{k}_\perp) = \Psi_{q\bar{q}}(x,k_\perp^2)$, has been implicitly adopted.

C. $F_{\pi\gamma}^{(NV)}(Q^2)$

As for $F_{\pi\gamma}^{(NV)}(Q^2)$, due to its nonperturbative nature, it is hard to be calculated in any Q^2 region. As stated in Ref. [14], around the region of $Q^2 \sim 0$, we can treat the photon inside the pion wave function (nearly on shell) as an external field that is approximately constant throughout the pion volume. And then, a fermion in a constant external field is modified only by a phase, i.e. $S_A(x-y) = e^{-ie(y-x)\cdot A}S_F(x-y)$. Consequently, the lowest $q\bar{q}$-wave function for the pion is modified only by a phase $e^{-iey\cdot A}$, where y is the $q\bar{q}$ separation. Transforming such phase into the momentum space and applying it to the wave function, we can obtain the two limiting behavior of $F_{\pi\gamma}^{(NV)}(Q^2)$ at $Q^2 \to 0$, which can be written as

$$F_{\pi\gamma}^{(NV)}(0) = F_{\pi\gamma}^{(V)}(0) = \frac{1}{8\sqrt{3}\pi^2}\int dx \Psi_{q\bar{q}}(x,\mathbf{0}_\perp), \quad (14)$$

and

$$\frac{\partial}{\partial Q^2}F_{\pi\gamma}^{(NV)}(Q^2)|_{Q^2\to 0} = \frac{1}{8\sqrt{3}\pi^2}\Big[\frac{\partial}{\partial Q^2}\int_0^1\int_0^{x^2Q^2}\Big(\frac{\Psi_{q\bar{q}}(x,k_\perp^2)}{x^2Q^2}\Big) \times dxdk_\perp^2\Big]_{Q^2\to 0} = \frac{-A}{128\sqrt{3}m^2\pi^2\beta^2}\int_0^1(1+B\times C_2^{3/2} \times (2x-1))\frac{x}{x'}(m^2+4xx'\beta^2) \times \exp\Big[-\frac{m^2}{8\beta^2xx'}\Big]dx, \quad (15)$$

where $x' = 1-x$. The above equation shows explicitly that at $Q^2 \to 0$, the leading Fock state contributes to $F_{\pi\gamma}(0)$ only half, i.e. $F_{\pi\gamma}^{(V)}(0) = F_{\pi\gamma}(0)/2$. While by taking both the valence and nonvalence contributions into consid-

TABLE II. Pion wave function parameters under the condition of $m_q = 0.30$ GeV, and its probability $P_{q\bar{q}}$, charged mean radius $\sqrt{\langle r_{\pi^+}^2\rangle^{q\bar{q}}}$ (unit fm), and the Gegenbauer moments $a_{2,4,6}(\mu_0^2)$.

B	A (GeV^{-1})	β (GeV)	$P_{q\bar{q}}$	$\sqrt{\langle r_{\pi^+}^2\rangle^{q\bar{q}}}$	$a_2(\mu_0^2)$	$a_4(\mu_0^2)$	$a_6(\mu_0^2)$
0.00	25.06	0.586	63.5%	0.341	0.027	−0.027	−0.016
0.20	21.71	0.641	60.0%	0.358	0.250	−0.025	−0.034
0.30	20.26	0.668	62.0%	0.378	0.362	−0.018	−0.041
0.40	18.91	0.695	66.1%	0.401	0.471	−0.008	−0.047
0.60	16.62	0.745	79.9%	0.451	0.679	0.020	−0.054

eration, one can get the correct rate of the process $\pi^0 \to \gamma\gamma$.

Next, we construct a phenomenological model for $F_{\pi\gamma}^{(NV)}(Q^2)$ by requiring that it satisfy the above listed two limiting behavior at $Q^2 = 0$ and by assuming that it is power suppressed to $F_{\pi\gamma}^{(V)}(Q^2)$ in the limit $Q^2 \to \infty$. For such purpose, we adopt the model constructed in Ref. [29]

$$F_{\pi\gamma}^{(NV)}(Q^2) = \frac{\alpha}{(1 + Q^2/\kappa^2)^2}, \tag{16}$$

where

$$\kappa = \sqrt{-\frac{F_{\pi\gamma}(0)}{\frac{\partial}{\partial Q^2} F_{\pi\gamma}^{(NV)}(Q^2)|_{Q^2\to 0}}}$$

and $\alpha = \frac{1}{2} F_{\pi\gamma}(0)$. It is easy to find that $F_{\pi\gamma}^{(NV)}(Q^2)$ will be suppressed by $1/Q^2$ to $F_{\pi\gamma}^{(V)}(Q^2)$ in the limit $Q^2 \to \infty$. Then at the large Q^2 region, the nonvalence Fock-state part $F_{\pi\gamma}^{(NV)}(Q^2)$ shall give a negligible contribution to the form factor. However it shall give a sizable contribution at the small Q^2 region.

D. Probability $P_{q\bar{q}}$ and charged mean square radius $\langle r_{\pi^+}^2 \rangle^{q\bar{q}}$

After deriving the possible ranges for the parameters in the pion wave function, we shall address the question of whether the resultant wave function and hence its DA is reasonable or not. In addition to the pion-photon transition form factor, the pion electromagnetic form factor $F_{\pi^+}(Q^2)$ also provides a platform for studying the properties of the pion wave function [34,40–43].

For such purpose, following the same procedure as described in detail in Ref. [34], we derive a formula for the soft part contribution by taking all the helicity components' contribution to the pion electromagnetic form factor. The general form for the soft part contribution can be written as [44]

$$F_{\pi^+}^s(Q^2) = \int \frac{dx d^2\mathbf{k}_\perp}{16\pi^3} \sum_{\lambda_1,\lambda_2} \Psi_{q\bar{q}}^*(x, \mathbf{k}_\perp, \lambda_1)\Psi_{q\bar{q}}(x, \mathbf{k}'_\perp, \lambda_2), \tag{17}$$

where $Q^2 = \mathbf{q}_\perp^2$ and $\mathbf{k}'_\perp = \mathbf{k}_\perp + (1 - x)\mathbf{q}_\perp$ for the final state light-cone wave function when taking the Drell-Yan-West assignment. We can derive the probability for finding the lowest valence quark state $P_{q\bar{q}}$ and the charged mean square radius $\langle r_{\pi^+}^2 \rangle^{q\bar{q}}$ from the limiting behavior of $F_{\pi^+}^s(Q^2)$ at $Q^2 \to 0$.

Substituting the pion model wave function (3) and finishing the integration over $\mathbf{k}_\perp$ with the help of the Schwinger α-representation method,

$$\frac{1}{A^\kappa} = \frac{1}{\Gamma(\kappa)} \int_0^\infty \alpha^{\kappa-1} e^{-\alpha A} d\alpha,$$

Eq. (17) can be simplified as

$$\begin{aligned} F_{\pi^+}^s(Q^2) = & \int_0^1 dx \int_0^\infty d\lambda \frac{A^2}{128\pi^2(1+\lambda)^3} \\ & \times \exp\left[-\frac{8m_q^2(1+\lambda)^2 + Q^2 x'^2(2+\lambda(4+\lambda))}{32x'x\beta^2(1+\lambda)}\right] \\ & \times [1 + B \times C_2^{3/2}(2x-1)]^2 \left\{ I_0\left(\frac{-Q^2x'\lambda^2}{32x\beta^2(1+\lambda)}\right) \right. \\ & \times [32x'x\beta^2(1+\lambda) - Q^2x'^2(2+\lambda(4+\lambda)) \\ & \left. + 8m_q^2(1+\lambda)^2] - I_1\left(\frac{-Q^2x'\lambda^2}{32x\beta^2(1+\lambda)}\right) Q^2x'^2\lambda^2 \right\}, \end{aligned} \tag{18}$$

where $x' = 1 - x$ and I_n $(n = 0, 1)$ stands for the modified Bessel function of the first kind. After taking the expansion in the small Q^2 limit, we obtain the probability $P_{q\bar{q}}$ for the valence quark state,

$$\begin{aligned} P_{q\bar{q}} = F_{\pi^+}^s(Q^2)|_{Q^2=0} &= \int \frac{dx d^2\mathbf{k}_\perp}{16\pi^3} |\Psi_{q\bar{q}}(x, \mathbf{k}_\perp)|^2 \\ &= \int_0^1 dx \int_0^\infty d\lambda \frac{A^2}{16\pi^2(1+\lambda)^2} [1 + B \times C_2^{3/2}(2x \\ &\quad - 1)]^2 \exp\left(-\frac{m_q^2(1+\lambda)}{4x'x\beta^2}\right) [m_q^2(1+\lambda) + 4xx'\beta^2] \end{aligned} \tag{19}$$

and the charged mean square radius $\langle r_{\pi^+}^2 \rangle^{q\bar{q}}$,

$$\begin{aligned} \langle r_{\pi^+}^2 \rangle^{q\bar{q}} &\approx -6 \frac{\partial F_{\pi^+}^s(Q^2)}{\partial Q^2}\Big|_{Q^2=0} \\ &= \int_0^1 dx \int_0^\infty d\lambda \frac{3A^2(2 + 4\lambda + \lambda^2)x'}{256\pi^2 x\beta^2(1+\lambda)^3} \\ &\quad \times [1 + B \times C_2^{3/2}(2x-1)]^2 \exp\left(-\frac{m_q^2(1+\lambda)}{4x'x\beta^2}\right) \\ &\quad \times [8x'x\beta^2 + m_q^2(1+\lambda)]. \end{aligned} \tag{20}$$

In the above two equations, one may observe that the terms in the second square brackets that are proportional to m_q^2 come from the ordinal helicity components, while the remaining terms in the same brackets are from the higher helicity components.

III. NUMERICAL RESULTS

We adopt the NLO $\alpha_s(Q^2)$ to do the numerical calculation, i.e.

$$\alpha_s(Q^2) = \frac{4\pi}{\beta_0 \ln(Q^2/\Lambda_{\rm QCD}^2)} \left[1 - \frac{2\beta_1}{\beta_0^2} \frac{\ln[\ln(Q^2/\Lambda_{\rm QCD}^2)]}{\ln(Q^2/\Lambda_{\rm QCD}^2)}\right], \tag{21}$$

where $\beta_0 = 11 - 2n_f/3$ and $\beta_1 = 51 - 19n_f/3$. The value of n_f varies with the energy scale and the value of

$\Lambda_{\rm QCD}$ is determined by requiring $\alpha_s(m_{Z^0}) = 0.1184$ [5], i.e. $\Lambda_{\rm QCD} = 0.231$ GeV.

A. Properties of pion wave function and pion DA

By taking $\mu_0 = 1$ GeV and $m_q = 0.30$ GeV, we present the wave-function parameters in Table II, which are determined by the mentioned constraints and by taking $B = 0.00$, 0.20, 0.30, 0.40, and 0.60, respectively. The probability for the valence quark state $P_{q\bar{q}}$, the charged mean radius $\sqrt{\langle r^2_{\pi^+}\rangle^{q\bar{q}}}$ (unit fm), and the Gegenbauer moments $a_{2,4,6}(\mu_0^2)$ are also presented in Table II. For the case of $B = 0$, $a_{2,4,6}(\mu_0^2)$ can be safely neglected due to their smallness, and then the corresponding DA is close to the asymptotic form as shown explicitly by Fig. 2. For a bigger B, it is found that $a_2(\mu_0^2)$ usually is much larger than $a_{4,6}(\mu_0^2)$, which is consistent with our model wave function (4), where only the first two Gegenbauer terms are kept in $\varphi(x)$. It is noted that by varying the parameter B within the region of $\sim[0.00, 0.60]$, the pion DA shall vary from aymptoticlike to a CZ-like form. To show this point more clearly, we draw the pion DA defined in Eq. (8) in Fig. 2, where $B = 0.00$, 0.30, and 0.60, respectively. As a comparison, we also present the conventional asymptotic-form DA, $\phi_{\rm AS}(x) = 6x(1-x)$ [4], and the CZ-form DA, $\phi_{\rm CZ}(x) = 30x(1-x)(2x-1)^2$ [17]. One may observe from Table II that the value of $\langle r^2_{\pi^+}\rangle^{q\bar{q}}$ increases with the increment of B, which runs within the region of $[(0.341\ \text{fm})^2, (0.451\ \text{fm})^2]$ by varying $B \in [0.00, 0.60]$. These values are somewhat smaller than the measured pion charged radius $\langle r^2\rangle^{\pi^+}_{\rm expt} = (0.657 \pm 0.012\ \text{fm})^2$ [45] and $(0.641\ \text{fm})^2$ [46], but it is close to the value as suggested in Refs. [34,47,48]. Such smaller $\langle r^2_{\pi^+}\rangle^{q\bar{q}}$ for the leading Fock-state wave function is reasonable, since the probability of leading Fock state $P_{q\bar{q}}$ is less than 1 and is about 60%–80%. This confirms the necessity of taking the higher Fock states into consideration to give full estimation of the pion electromagnetic form factor/pion-photon transition form factor, especially for lower Q^2 regions.

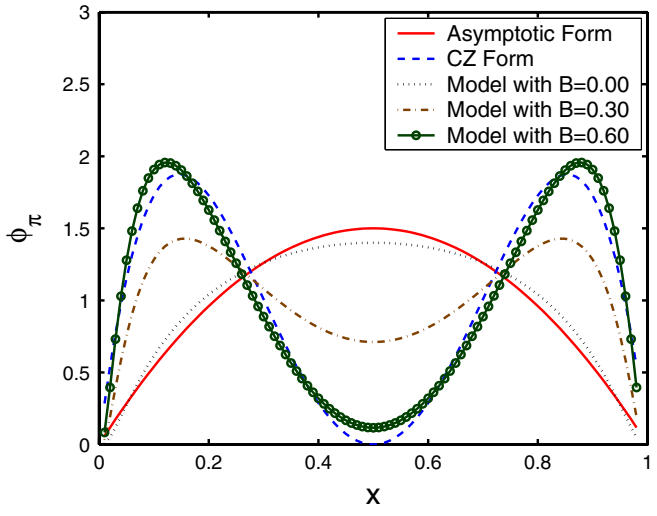

FIG. 2 (color online). Comparison of the pion DA model defined in Eq. (8) with the asymptotic-form DA and the CZ-form DA, where $B = 0.00$, 0.30, and 0.60, respectively.

A naive pion wave-function model has been suggested in Ref. [10] to explain the new *BABAR* data [3], which is constructed with a flat DA together with a Gaussian ansatz for the $k_\perp$ dependence, i.e.

$$\Psi_{q\bar{q}}(x, \mathbf{k}_\perp) = \frac{4\pi^2 f_\pi \phi_\pi(x)}{\sqrt{3}xx'\sigma} \exp\Big(-\frac{k_\perp^2}{2\sigma xx'}\Big), \tag{22}$$

where $x' = 1 - x$ and $\phi_\pi(x) \equiv 1$. With such a model (by setting $\sigma = 0.53\ \text{GeV}^2$), it can be easily seen that one cannot derive the right behavior at $Q^2 \to 0$ [10], since following similar steps as shown in Sec. II D, it will lead to

$$P_{q\bar{q}} = \int_0^1 \Big(\frac{\pi^2 f_{pi}^2}{3xx'\sigma}\Big) dx$$

and

$$\langle r^2_{\pi^+}\rangle^{q\bar{q}} = \int_0^1 \Big(\frac{\pi^2 f_\pi^2}{2x^2\sigma^2}\Big) dx,$$

both of which are divergent. This in some sense explains why such a model wave function can explain the pion-photon transition form factor's large Q^2 behavior (due to the large enhancement at the end-point region), but fails to explain the lower Q^2 behavior.

Next, it would be interesting to make a comparison with Brodsky and Teramond's (BT) holographic model with a quark mass effect [49,50] for the pion DA. The BT model is predicted by using the anti–de Sitter/conformal field theory (AdS/CFT) correspondence and by using the soft-wall holographic model, whose explicit form is [50]

$$\phi_M(x, \mu_0^2) = \mathcal{C}\sqrt{x(1-x)} \exp\Big[-\frac{1}{2\kappa^2}\Big(\frac{m_u^2}{x} + \frac{m_d^2}{1-x}\Big)\Big] \times \Big[1 - \exp\Big(-\frac{\mu_0^2}{2\kappa^2 x(1-x)}\Big)\Big], \tag{23}$$

where $\kappa = 0.375$ GeV [49], $m_u = 2$ MeV, and $m_d = 5$ MeV [50]. The factor $\mathcal{C} \simeq 2.55$, which can be determined by its normalization. It is found that for $\mu_0 \sim 1$ GeV, the term involving μ_0 gives a quite small contribution and it can be safely neglected as is done by Ref. [50]. A comparison of our present pion DA model (8) with that of the BT model is presented in Fig. 3, where our models with $B = 0.00$, 0.05, 0.10, and 0.15 are presented by the circles, the dashed, the dash-dotted, and dotted lines, respectively, and the BT model is drawn by a solid line. Since both models have similar transverse momentum behavior, it is natural to estimate that when setting $B \simeq 0.125$, which corresponds to the same second Gegenbauer moment of the BT model $a_2(\mu_0^2) \sim 0.145$. These two models shall lead to a similar behavior for the pion-photon transition

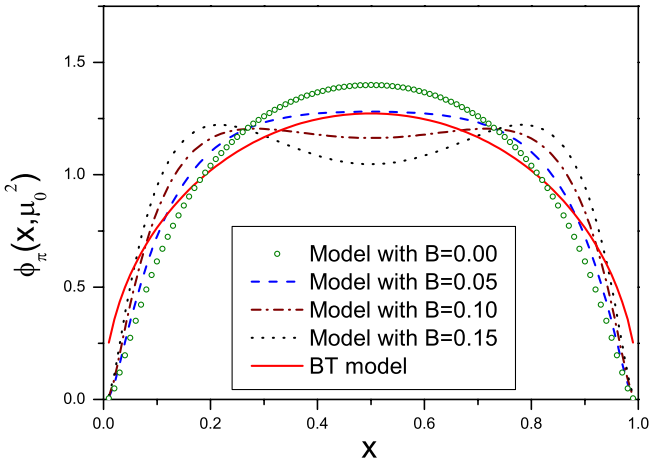

FIG. 3 (color online). Comparison of the pion DA model defined in Eq. (8) with Brodsky and Teramond's (BT) holographic model, where $B = 0.00$, 0.05, 0.10, and 0.15, respectively.

form factor if calculating under the calculation technology as described in Sec. II C.[2]

B. Pion-photon transition form factor

First, we calculate the pion-photon transition form factor with the model wave function (3) by taking $m_q = 0.30$ GeV and by varying B within the region of [0.00, 0.60]. The result is shown in Fig. 4, where the dash-dotted line, the dotted line, and the dashed line are for $B = 0.00$, $B = 0.30$, and $B = 0.60$, respectively. As a comparison, we also present the *BABAR* fitted curve (1) in Fig. 4, which is shown by a solid line. For a small energy region, $Q^2 \lesssim 15$ GeV^2, it is found that both asymptoticlike and CZ-like wave functions by adjusting the quark mass parameter can explain the CELLO, CLEO, and *BABAR* experimental data, which agrees with the observation in Ref. [29]. However, at large Q^2 region, different behavior of DA (by varying B) shall lead to different limiting behavior. Typically, it is found that when $Q^2 \to \infty$, the $Q^2 F_{\pi\gamma}(Q^2)$ for asymptoticlike wave function (with $B = 0$) tends to the usual limit $2f_\pi \simeq 0.185$ GeV [4]. So to explain the newly obtained *BABAR* data on the high energy region, we need a broader DA other than the asymptotic one. It is found that with the increment of B (corresponding to a more broader DA as shown by Fig. 2), the estimated pion-transition form factor shall be closer to the *BABAR* data. Therefore the pion DA behavior will be determined, if the *BABAR* present measurement can be confirmed in the coming future.

[2]For such a calculation, one needs to be careful that the spin-space wave function for the BT model should be changed accordingly, since m_u and m_d are taken as different values that are different from our present treatment of $m_u = m_d = m_q$.

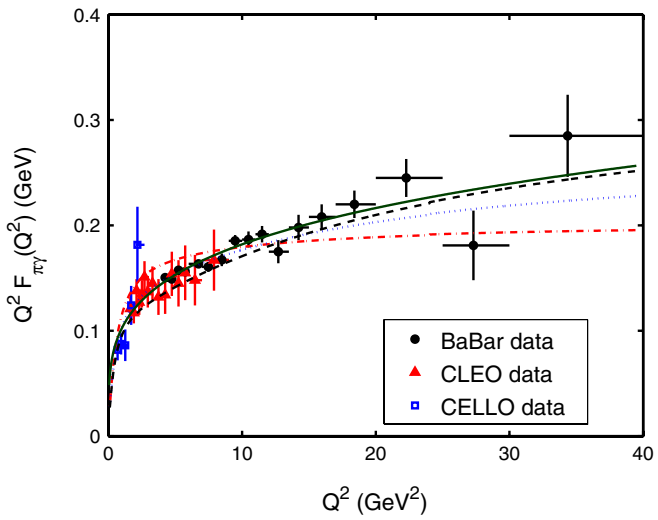

FIG. 4 (color online). $Q^2 F_{\pi\gamma}(Q^2)$ with the model wave function (3) by taking $m_q = 0.30$ GeV and by varying B within the region of [0.00, 0.60]. The dash-dotted, the dotted, and the dashed lines are for $B = 0.00$, $B = 0.30$, and $B = 0.60$, respectively. The solid line is the fitted curve (1) derived by *BABAR* [3].

Second, we show how the leading valence quark and the nonvalence quark contribute to the pion-photon transition form factor. We show the results for $B = 0.60$ in Fig. 5, where the solid line, the dotted line, and the dashed line are for the total contribution, the leading valence quark contribution, and the nonvalence quark contribution to the pion-photon transition form factor, respectively. Figure 5 shows that the leading valence Fock-state contribution dominates the pion-photon transition from factor

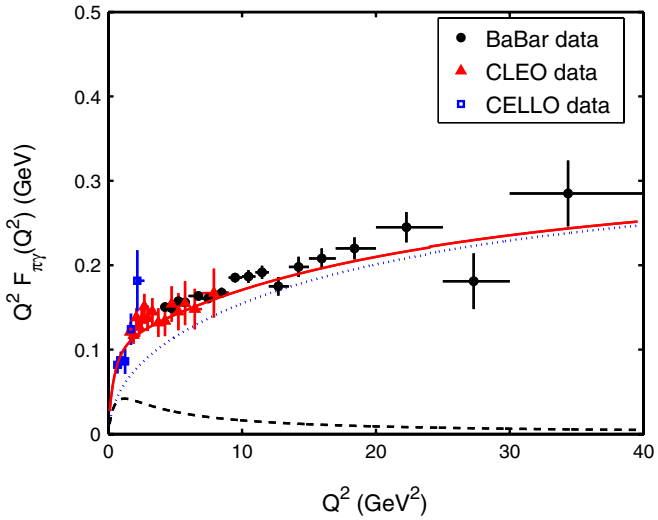

FIG. 5 (color online). $Q^2 F_{\pi\gamma}(Q^2)$ with the model wave function (3) by taking $m_q = 0.30$ GeV and $B = 0.60$. The solid, the dotted, and the dashed lines are for the total contribution, the leading valence quark contribution, and the nonvalence quark contribution to the form factor, respectively.

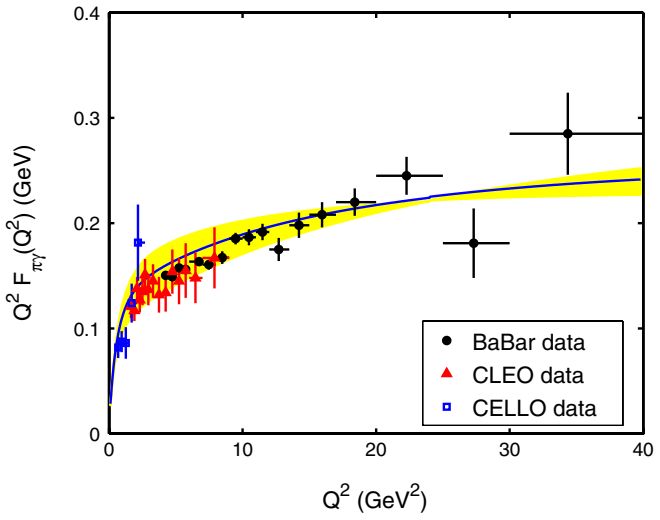

FIG. 6 (color online). $Q^2F_{\pi\gamma}(Q^2)$ with the model wave function (3) by fixing $B = 0.60$ and by varying m_q within the region [0.30, 0.50] GeV. The solid line is for $m_q = 0.40$ GeV, and the shaded band shows its uncertainty.

$Q^2F_{\pi\gamma}(Q^2)$ for the large Q^2 region, and the nonvalence quark part is small in the high Q^2 region, but it shall provide a sizable contribution to the low and intermediate energy regions. So one should consider the nonvalence Fock-states' contribution to $Q^2F_{\pi\gamma}(0)$ so as to explain the experimental data at both low and high Q^2 regions.

Third, we discuss the uncertainties caused by varying the value of m_q. For such purpose, we fix B to be 0.60.[3] From Fig. 2, one may observe that when $B = 0.6$, the DA is close to the CZ form. As has been argued in Ref. [29], for the case of CZ-like DA, in order to be consistent with the experimental data at low energy scale, m_q should be within the region of $0.40^{+0.10}_{-0.10}$ GeV. So we vary m_q within the region of [0.30, 0.50] GeV to show the uncertainties. The results are shown in Fig. 6, where the solid line is for $m_q = 0.40$ GeV, and the shaded band shows its uncertainty. In the lower Q^2 region, the upper edge of the band is for $m_q = 0.50$ GeV and the lower edge is for $m_q = 0.30$ GeV; while in the higher Q^2 region, the upper edge of the band is for $m_q = 0.30$ GeV and the lower edge is for $m_q = 0.50$ GeV.

[3]The case of $B = 0.30$ is similar, only the range of m_q should be shifted to $0.30^{+0.10}_{-0.10}$ GeV [29].

IV. SUMMARY

In the present paper, we have taken both the valence quark states and the nonvalence quark states into consideration. The valence quark part is calculated up to NLO within the k_T factorization approach and the nonvalence quark part is estimated by a naive model based on its limiting behavior at both $Q^2 \to 0$ and $Q^2 \to \infty$. Our results show that (1) For $Q^2 \lesssim 15$ GeV^2, it is found that both asymptoticlike and broader wave functions can explain the CELLO, CLEO, and *BABAR* experimental data under reasonable choices of parameters. To be consistent with the new *BABAR* data at the large Q^2 region, we need a broader DA, i.e. the conventional adopted asymptotic DA should be broadened to a certain degree. (2) With suitable parameters for the pion model wave function that is constructed based on the BHL prescription, it is found that a more broader DA (with larger B) shall lead to a better agreement with the *BABAR* data. If *BABAR* confirms its present measurement, then pion DA should be broader, such as a CZ-like one with an improved behavior at the end-point region. (3) The present adopted model of the pion wave function as shown by Eq. (4) shall present a basis for the application of the pQCD approach [4,40–43].

ACKNOWLEDGMENTS

The authors would like to thank Dr. Fen Zuo and Dr. Ming-Zhen Zhou for helpful discussions. This work was supported in part by the Natural Science Foundation of China under Grants No. 10975144, No. 10735080, and No. 10805082, and by the Natural Science Foundation Project of CQ CSTC under Grant No. 2008BB0298, and by the Fundamental Research Funds for the Central Universities under Grant No. CDJZR101000616.

[1] H.-J. Behrend *et al.* (CELLO Collaboration), Z. Phys. C **49**, 401 (1991).
[2] V. Savinov *et al.*, (CLEO Collaboration), arXiv:hep-ex/9707028; J. Gronberg *et al.* (CLEO Collaboration), Phys. Rev. D **57**, 33 (1998).
[3] B. Aubert *et al.*, (*BABAR* Collaboration), Phys. Rev. D **80**, 052002 (2009).
[4] G. P. Lepage and S. J. Brodsky, Phys. Rev. D **22**, 2157 (1980).
[5] C. Amsler *et al.* (Particle Data Group), Phys. Lett. B **667**, 1 (2008).
[6] F. Del Aguila and M. K. Chase, Nucl. Phys. **B193**, 517 (1981); E. Braaten, Phys. Rev. D **28**, 524 (1983); E. P. Kadantseva, S. V. Mikhailov, and A. V. Radyushkin, Yad. Fiz. **44**, 507 (1986) [Sov. J. Nucl. Phys. **44**, 326 (1986)].
[7] B. Melic, B. Nizic, and K. Passek, Phys. Rev. D **65**, 053020 (2002).
[8] B. Melic, D. Muller, and K. Passek-Kumericki, Phys. Rev. D **68**, 014013 (2003).
[9] S. V. Mikhailov and N. G. Stefanis, Nucl. Phys. **B821**, 291

(2009).
[10] A. V. Radyushkin, Phys. Rev. D **80**, 094009 (2009).
[11] M. V. Polyakov, JETP Lett. **90**, 228 (2009).
[12] S. Nogeura and V. Vento, arXiv:1001.3075.
[13] A. E. Dorokhov, arXiv:1003.4693.
[14] S. J. Brodsky, T. Huang, and G. P. Lepage, in *Proceedings of the Banff Summer Institute, Banff, Alberta, 1981*, edited by A. Z. Capri and A. N. Kamal (Plenum, New York, 1983), p. 143; T. Huang, in *Proceedings of the XXth International Conference on High Energy Physics, Madison, Wisconsin, 1980*, edited by L. Durand and L. G. Pondrom, AIP Conf. Proc. No. 69 (AIP, New York, 1981), p. 1000.
[15] H. N. Li and S. Mishima, Phys. Rev. D **80**, 074024 (2009).
[16] T. Kurimoto, H. N. Li, and A. I. Sanda, Phys. Rev. D **65**, 014007 (2001); C. D. Lu and M. Z. Yang, Eur. Phys. J. C **28**, 515 (2003); T. Huang and X. G. Wu, Phys. Rev. D **71**, 034018 (2005), and reference therein.
[17] V. L. Chernyak and A. R. Zhitnitsky, Nucl. Phys. **B201**, 492 (1982).
[18] E. R. Arriola and W. Broniowski, Phys. Rev. D **66**, 094016 (2002).
[19] V. M. Braun, A. Khodjamirian, and M. Maul, Phys. Rev. D **61**, 073004 (2000).
[20] A. P. Bakulev, S. V. Mikhailov, and N. G. Stefanis, Phys. Lett. B **578**, 91 (2004); A. P. Bakulev, K. Passek-Kumericki, W. Schroers, and N. G. Stefanis, Phys. Rev. D **70**, 033014 (2004); **70**, 079906(E) (2004); A. P. Bakulev, S. V. Mikhailov, and N. G. Stefanis, Phys. Rev. D **67**, 074012 (2003); **73**, 056002 (2006).
[21] P. Ball and R. Zwicky, Phys. Lett. B **625**, 225 (2005).
[22] Seung-il Nam, Hyun-Chul Kim, Atsushi Hosaka, and M. M. Musakhanov, Phys. Rev. D **74**, 014019 (2006).
[23] S. S. Agaev, Phys. Rev. D **72**, 114010 (2005); **73**, 059902(E) (2006).
[24] X. G. Wu, Eur. Phys. J. C **57**, 665 (2008).
[25] L. Del Debbio, M. Di Perro, and A. Dougall, Nucl. Phys. B, Proc. Suppl. **119**, 416 (2003).
[26] M. Gockeler *et al.*, Nucl. Phys. B, Proc. Suppl. **161**, 69 (2006).
[27] S. Dalley and Brett van de Sande, Phys. Rev. D **67**, 114507 (2003).
[28] B. Aubert *et al.* (*BABAR* Collaboration), arXiv:hep-ex/0607060.
[29] T. Huang and X. G. Wu, Int. J. Mod. Phys. A **22**, 3065 (2007).
[30] A. V. Radyushkin, Acta Phys. Pol. B **26**, 2067 (1995); arXiv:hep-ph/9511272.
[31] H. J. Melosh, Phys. Rev. D **9**, 1095 (1974).
[32] T. Huang, B. Q. Ma, and Q. X. Shen, Phys. Rev. D **49**, 1490 (1994).
[33] F. G. Cao and T. Huang, Phys. Rev. D **59**, 093004 (1999).
[34] T. Huang and X. G. Wu, Phys. Rev. D **70**, 093013 (2004); X. G. Wu and T. Huang, Int. J. Mod. Phys. A **21**, 901 (2006).
[35] T. Huang and X. G. Wu, Int. J. Mod. Phys. A **22**, 3065 (2007).
[36] G. P. Lepage and S. J. Brodsky, Phys. Lett. **87B**, 359 (1979); Phys. Rev. Lett. **43**, 545 (1979); Phys. Rev. D **22**, 2157 (1980).
[37] Fu-Guang Cao, Tao Huang, and Bo-Qiang Ma, Phys. Rev. D **53**, 6582 (1996).
[38] I. V. Musatov and A. V. Radyushkin, Phys. Rev. D **56**, 2713 (1997).
[39] S. Nandi and H. N. Li, Phys. Rev. D **76**, 034008 (2007).
[40] T. Huang and Q. X. Sheng, Z. Phys. C **50**, 139 (1991); F. G. Cao, J. Cao, T. Huang, and B. Q. Ma, Phys. Rev. D **55**, 7107 (1997).
[41] H. N. Li and G. Sterman, Nucl. Phys. **B381**, 129 (1992); J. Botts and G. Sterman, Nucl. Phys. **B325**, 62 (1989); F. G. Cao, T. Huang, and C. W. Luo, Phys. Rev. D **52**, 5358 (1995).
[42] A. Szczepaniak, C. R. Ji, and A. Radyushkin, Phys. Rev. D **57**, 2813 (1998).
[43] C. R. Ji, A. Pang, and A. Szczepaniak, Phys. Rev. D **52**, 4038 (1995).
[44] S. D. Drell and T. M. Yan, Phys. Rev. Lett. **24**, 181 (1970).
[45] S. R. Amendolia *et al.*, Phys. Lett. **146B**, 116 (1984); Nucl. Phys. **B277**, 168 (1986).
[46] G. M. Huber *et al.* (Jefferson Lab Collaboration), Phys. Rev. C **78**, 045203 (2008).
[47] B. Povh and J. Hufner, Phys. Lett. B **245**, 653 (1990); T. Huang, Nucl. Phys. B, Proc. Suppl. **7**, 320 (1989).
[48] W. Wilcox and R. M. Woloshyn, Phys. Rev. Lett. **54**, 2653 (1985).
[49] S. J. Brodsky and Guy F. de Teramond, Phys. Rev. Lett. **96**, 201601 (2006); Phys. Rev. D **77**, 056007 (2008).
[50] S. J. Brodsky and Guy F. de Teramond, arXiv:0802.0514.